Available online at www.sciencedirect.com
ScienceDirect
Carbohydrate Research 342 (2007) 1910–1917
Carbohydrate RESEARCH

Conformational behaviour of glycomimetics: NMR and molecular modelling studies of the C-glycoside analogue of the disaccharide methyl β-D-galactopyranosyl-(1→3)-β-D-glucopyranoside

Paloma Vidal,[a] Boris Vauzeilles,[b,c] Yves Blériot,[d,e] Matthieu Sollogoub,[d,e] Pierre Sinaÿ,[d,e] Jesús Jiménez-Barbero[f,*] and Juan F. Espinosa[a,*]

[a]*Discovery Chemistry Research and Technologies, Centro de Investigación Lilly, Avenida de la Industria 30, 28108 Alcobendas, Madrid, Spain*
[b]*CNRS, Institut de Chimie Moléculaire et des Matériaux d'Orsay, UMR8182, Orsay F-91405, France*
[c]*Université Paris-Sud, Orsay F-91405, France*
[d]*École Normale Supérieure, Département de Chimie, UMR CNRS 8642, 24, rue Lhomond, 75231 Paris Cedex 05, France*
[e]*Université Pierre et Marie Curie-Paris 6, Institut de Chimie Moléculaire (FR 2769), 75005 Paris, France*
[f]*Departamento de Estructura y Función de Proteínas, Centro de Investigaciones Biológicas, CSIC, Ramiro de Maeztu 9, 28040 Madrid, Spain*

Received 9 February 2007; received in revised form 16 April 2007; accepted 24 April 2007
Available online 29 April 2007

Abstract—The conformational behaviour of the C-glycoside β-C-Gal-(1→3)-β-Glc-OMe (**1**) has been studied using a combination of molecular mechanics and NMR spectroscopy (proton–proton coupling constants and nuclear Overhauser effects). It is shown that the C-disaccharide populates two distinctive conformational families in solution, the normal *syn-ψ* conformation, which is the predominating conformation of parent O-glycoside **2**, and the *anti-ψ* conformation, which has not been detected for the O-disaccharide.

Keywords: C-Glycosides; Conformational analysis; Glycomimetics

1. Introduction

The search for new glycomimetics has led to a group of compounds denoted C-glycosides, in which the anomeric oxygen atom has been replaced by a methylene group.[1] The determination of the three-dimensional structure of C-glycosides and its comparison with that of O-glycosides is of primary importance to evaluate the potential of the C-analogues as glycosidase inhibitors. Kishi and co-workers, based mainly on the analysis of proton–proton coupling constants, have concluded that both types of compounds exhibit similar conformational properties in solution.[2] However, a detailed conformational analysis of a number of C-disaccharides has revealed that the conformational similarity between the O- and C-glycosides is not a general phenomenon.[3] For instance, C-lactose and C-mannobiose present significant differences relative to their parent O-glycosides.[4] These findings have encouraged us to extend the comparison between C- and O-glycosides to other linkages. Here, we now report the conformational analysis of the C-disaccharide β-C-Gal-(1→3)-β-Glc-OMe[5] (**1**) in water and methanol using NMR spectroscopy in tandem with molecular mechanics calculations, and the comparison with the parent O-disaccharide (**2**). The β-

* Corresponding authors. E-mail addresses: jjbarbero@cib.csic.es; jfespinosa@lilly.com

0008-6215/$ - see front matter © 2007 Elsevier Ltd. All rights reserved.
doi:10.1016/j.carres.2007.04.017

(1→3)-linkage is present in some of the histo-blood group carbohydrate antigens,[6] specifically in H types 1, 3 and 4, A type 1, Lewis A and B, and in the disaccharide β-laminarabiose, which is the repeating unit of fungal β-(1→3)-glucans that have antitumoural and immunomodulatory properties.[7]

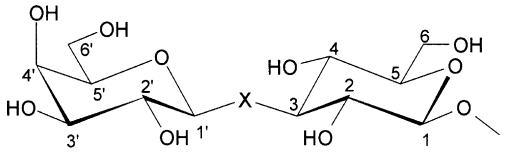

1 X = CH_2
2 X = O

2. Results and discussion

The protocol used to deduce the conformational behaviour of **1** and **2**, which has been described,[4] involves the calculation of the conformational energy maps by molecular mechanics calculations, followed by the determination of the expected NMR parameters, vicinal proton–proton couplings (J) and nuclear Overhauser effects (NOE) from the population distribution, and the comparison with the experimental data to validate the theoretical results. Three staggered conformations around the glycosidic bond are possible, which have been termed *exo-syn* (60°), *exo-anti* (180°) or non-*exo* (−60°), by considering their accordance with the *exo*-anomeric geometry and their disposition in a *syn*- or *anti*-type arrangement. Regarding the aglyconic bond, the three staggered conformations are denoted as *syn*-(+), *syn*-(−) and *anti*, corresponding to dihedral angle values of 60°, −60° and 180°, respectively, although an eclipsed orientation *syn*-(eclipsed) may also occur.

2.1. Molecular mechanics calculations

The energy maps of **1** and **2** as a function of the glycosidic (ϕ) and aglyconic (ψ) torsions were built using the MM3* force field.[8] The dihedral angles were defined as ϕ(H1′–C1′–X–C3) and ψ(C1′–X–C3–H3). Four relaxed energy maps were calculated to take into account different orientations for the hydroxymethyl group. The adiabatic surfaces built from the relaxed maps along with the probability distributions obtained according to Boltzmann functions are shown in Figure 1. The relative populations as a function of ϕ and ψ are shown in Figure 2.

For O-glycoside **2**, about 98% of the population is located in the central low-energy region represented by global minimum A, which belongs to the *syn*-ϕ/*syn*-ψ conformational family (Table 1). The *anti*-ψ minimum B and the *anti*-ϕ minimum C are barely predicted by the calculations (about 1% of each conformer). These results are consistent with previous computational studies performed for β-(1→3) linkages. For instance, the MM3[9] energy maps of β-laminarabiose (β-Glc-(1→3)-β-Glc) and β-Gal-(1→3)-β-GlcNAc are very similar to that of **2**.[10] More recently, the conformational behaviour around the β-(1→3) linkage of β-laminarabiose was investigated in detail through molecular dynamics (MD) simulations in water.[11] The dihedral angles exhibited a rather low degree of flexibility and the trajectory remained in the central lowest energy region. The analysis of a set of crystallographic structures of oligosaccharides containing the β-(1→3) linkage revealed that the molecules adopted *syn*-ϕ/*syn*-ψ conformations in the solid state, in agreement with the theoretical results.[12] Also, the conformational preferences around this linkage have been investigated in solution through NMR spectroscopy. The application of quantitative NOE measurements for Lewis a and Lewis b determinants showed that only the *syn*-ϕ/*syn*-ψ orientations of the β-Gal-(1→3)-β-GlcNAc linkage produced simulated spectra agreeing to the NOESY spectra.[13] Moreover, the ϕ and ψ dihedral angles derived from the $^3J_{H1',C3}$and $^3J_{C1',H3}$ coupling constants[14] for β-laminarabiose are consistent with the predominance of the *syn*-ϕ/*syn*-ψ conformation.[15] Nevertheless, unambiguous experimental evidence for the existence of the *anti*-ψ conformation in DMSO solution was provided for the β-Gal-(1→3)-β-Glc-OMe disaccharide through the detection of a diagnostic hydrogen bond in a partially deuterated sample.[16]

The analysis of the distribution map of C-glycoside **1** reveals the presence of five low-energy conformations (Fig. 3). Again, the *syn*-ϕ/*syn*-ψ conformational family is the most populated, accounting for 72% of the population. This lowest energy region is centred around $\phi =$ 60° and defined by ψ values between 90° and −90°. Two minima are located in this area, the global minimum A and a local minimum D with a relative energy of approximately 1 kcal/mol. These minima correspond to the *syn*-ψ(+) and *syn*-ψ(−) staggered conformations, respectively. A small population (about 3%) of the non-*exo* conformation not detected for the parent O-glycoside due to the occurrence of the *exo*-anomeric effect is also predicted (minimum E). Remarkably, the calculations indicate that the *syn*-ϕ/*anti*-ψ conformational family, in contrast to O-disaccharide **2**, is populated significantly in solution, with 24% of the population concentrated around minimum B. The calculations suggest that C-disaccharide **1** presents the same conformational preference around the glycosidic bond as its parent O-disaccharide (*exo*-anomeric conformation), but more conformational diversity around the aglyconic bond. Similar conclusions were reported by Mikros et al. on the basis of their MM3 calculations ($\varepsilon = 4$) of the C-analogue of β-laminarabiose.[17] According to their calculations, the relative energy of the *anti*-ψ conformer with respect to the most stable *syn*-ψ conformer for the

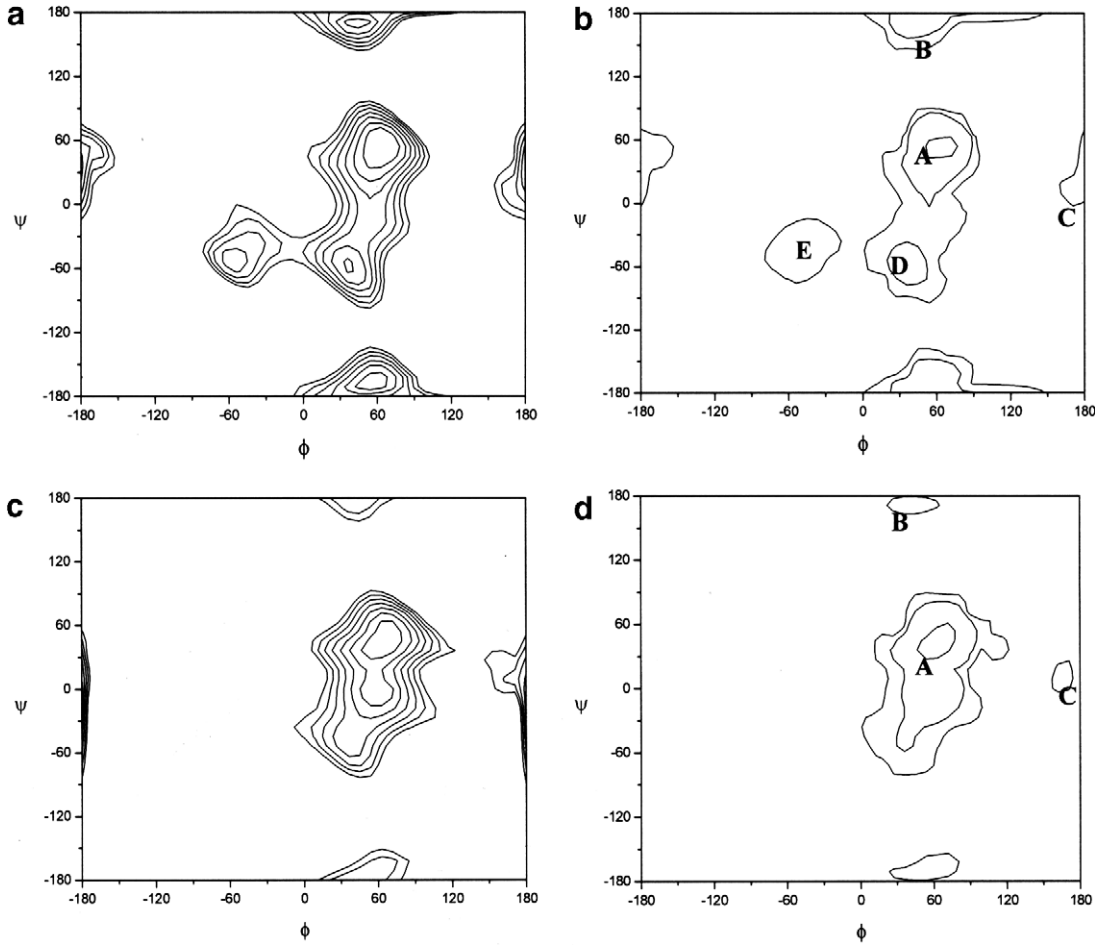

Figure 1. Adiabatic (a, c) and population distribution (b, d) maps for **1** (a, b) and **2** (c, d). Energy contours are given every 0.5 kcal/mol. Distribution contours are given at 10%, 1% and 0.1% of the population.

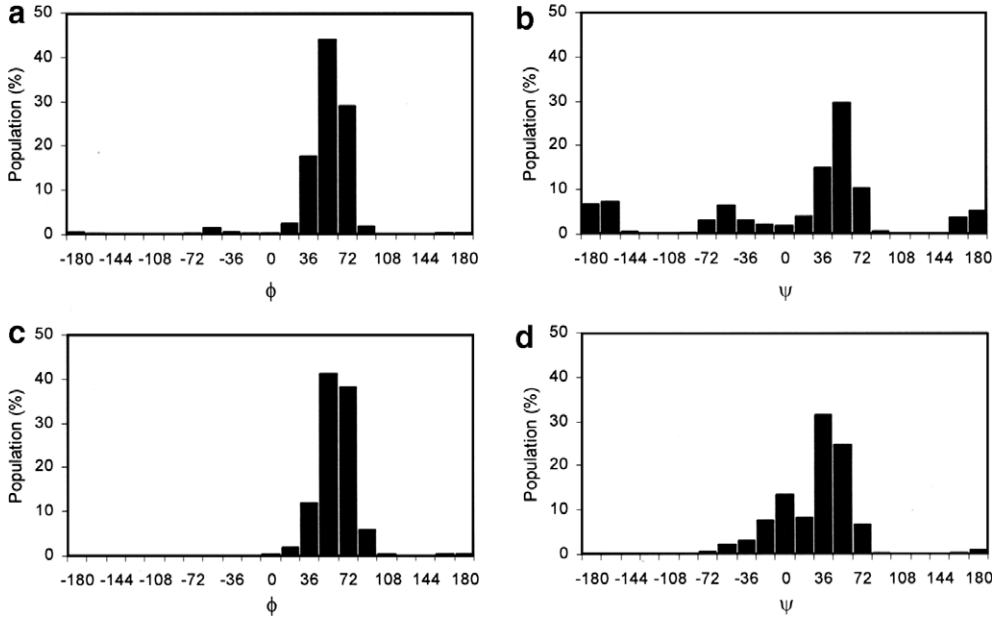

Figure 2. Relative populations of **1** (a, b) and **2** (c, d) as a function of the dihedral angles ϕ (a, c) and ψ (b, d).

Table 1. Torsion angle values and relative MM3* energies of the predicted minima and populations (%) of the low-energy regions

Minima	Torsions (ϕ/ψ)	Pop. (%)	Type (ϕ)	Type (ψ)
Compound **1**				
A	57/25	98	*exo-syn*	*syn*
B	41/168	1	*exo-syn*	*anti*
C	165/16	1	*exo-anti*	*syn*
Compound **2**				
A	65/56	60	*exo-syn*	*syn*-(+)
B	45/176	24	*exo-syn*	*anti*
C	−171/53	1	*exo-anti*	*syn*-(+)
D	38/−59	12	*exo-syn*	*syn*-(−)
E	−57/−54	3	non-*exo*	*syn*-(−)

The conformational families of the minima are indicated.

O-disaccharide is 3.6 kcal/mol and, therefore, only the latter conformational family would exist in solution. In contrast, the relative energy between both conformers for the C-analogue is 1.1 kcal/mol, implying that the *anti*-ψ conformational family should also be populated in solution.

2.2. NMR spectroscopy

The validity of the theoretical results was verified for **1** through NMR spectroscopy. The ^{1}H NMR spectrum in D_2O was assigned using a combination of COSY and HSQC experiments (Table 2). The diastereotopic assignment of the prochiral HpR and HpS protons of the methylene bridge was performed using a protocol similar to that described previously, based exclusively on a combination of J and NOEs values.[4c] The intra-ring vicinal proton–proton coupling constants proved that the six-membered rings adopt the $^4C_1$ chair conformation. The major advantage of the conformational studies of C-glycosides with respect to O-glycosides is that four proton–proton coupling constants across the pseudo-glycosidic linkage can be measured and converted into dihedral angles through the well-established Karplus–Altona equation.[18] Second-order analysis of the spectrum was performed to obtain refined values for these couplings (Fig. 4).

The experimental couplings can be compared with the calculated values for minima A–E and for the ensemble average (Table 3). The small $^3J_{H1'-HpS}$ value reveals that the non-*exo* conformer is barely populated in solution because this geometry places H1′ and HpS in an *anti* disposition and a higher coupling constant would be expected if this conformer was populated appreciably in solution. Analogously, the large $^3J_{H1'-HpR}$ value discards the presence of a significant population of the *anti*-ϕ conformer that arranges H1′ and HpR in a *gauche* relationship. Both conclusions are consistent

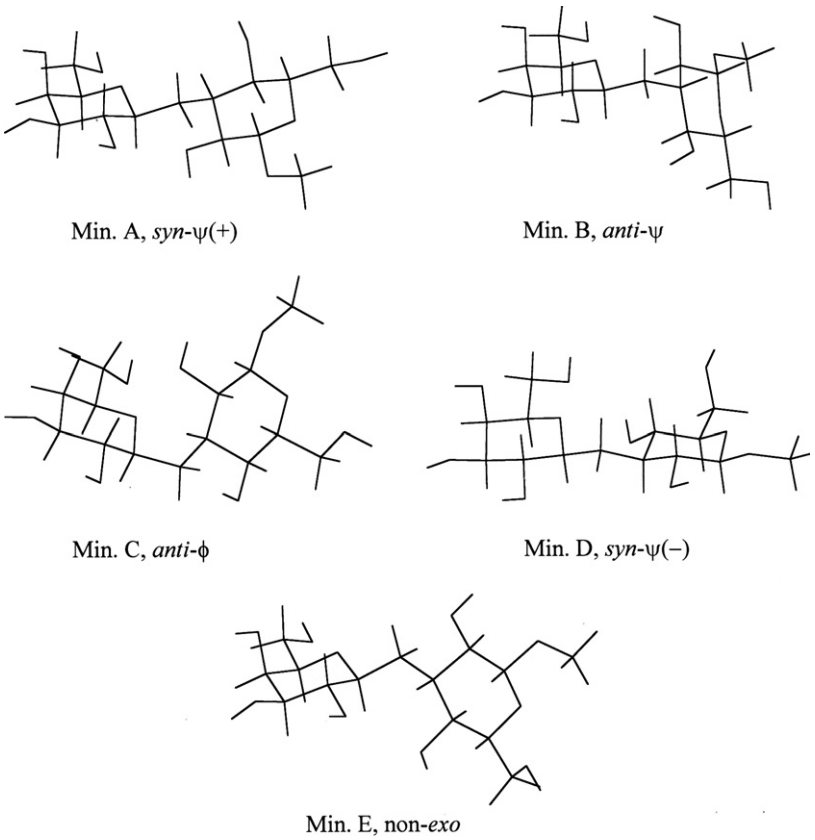

Figure 3. Views of the major low-energy conformations obtained by MM3* calculations for C-disaccharide **1**.

Table 2. ^{1}H and ^{13}C NMR chemical shifts (δ, ppm) of 1 in D_2O and CD_3OD at 298 K

	D_2O		CD_3OD			D_2O		CD_3OD	
	^{1}H	^{13}C	^{1}H	^{13}C		^{1}H	^{13}C	^{1}H	^{13}C
1′	3.45	81.5	3.40	80.4	1	4.33	107.6	4.15	106.6
2′	3.42	74.1	3.42	72.8	2	3.31	75.2	3.15	73.9
3′	3.60	76.7	3.44	75.9	3	1.80	47.7	1.69	46.9
4′	3.94	72.0	3.84	70.7	4	3.31	70.7	3.21	70.1
5′	3.62	81.3	3.48	80.1	5	3.47	81.5	3.31	80.5
6′a	3.72	64.0	3.73	62.9	6a	3.91	64.2	3.87	62.7
6′b	3.69		3.67		6b	3.69		3.64	
pS	2.23	33.4	2.34	33.1	Me	3.55	59.8	3.53	56.9
pR	1.79		1.76						

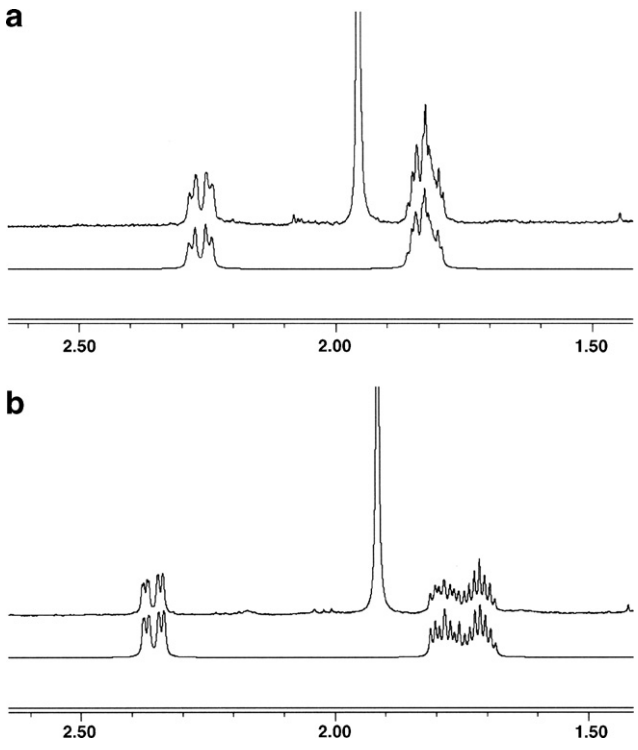

Figure 4. Expansions of the low-frequency region of the experimental ^{1}H spectra (top traces) of **1** in D_2O (a) and CD_3OD (b) together with the simulated spectra (bottom traces). The singlet peak arises from residual acetone.

with MM3* calculations that predict very low populations for both regions of the conformational map. Basically, the extreme values for the two coupling constants across ϕ bond confirm that **1** adopts predominantly the *exo-syn* conformation around the glycosidic bond, as do regular O-glycosides. In contrast, the intermediate values for the two couplings across the ψ bond ($^{3}J_{H3–HpS}$ and $^{3}J_{H3–HpR}$) reflect the existence of significant conformational averaging around the C-aglyconic torsion, which is consistent with the coexistence of the *syn*-ψ and *anti*-ψ conformational families predicted by the calculations. Satisfactory agreement between the experimental and the theoretical couplings for the distribution is obtained (Table 3). A clear difference between the calculated and the measured values is observed, however, for the $J_{H3–HpS}$ coupling constant. The ensemble average value is higher than the experimental value, suggesting that the population of the *syn*-ψ(+) conformation, which arranges both protons in an *anti* disposition, is overestimated by the calculations.

Further structural information can be extracted from NOESY and ROESY experiments to complement the coupling constants data. Unfortunately, the measurement of NOE intensities in D_2O was hampered by the existing signal overlapping. This issue is usually less severe in C-glycosides relative to O-glycosides as a consequence of the shielding effect of the methylene group bridging the rings. However, considerable overlapping of signals is still observed in **1**: two key resonances, H2 and H4, appear at the same chemical shifts, and H3 and HpR signals are partially overlapped. A variety of temperatures were explored in an attempt to overcome this situation, but with no success. Finally, the NMR studies were undertaken in a second solvent, CD_3OD, in which a better signal dispersion was observed. Although some changes in the relative population of the conformers might be expected between the two solvents, the fact that the coupling constants across

Table 3. Experimental vicinal coupling constants ($^{3}J_{HH}$) across the C1′–CH_2–C3 bridge of 1 in D_2O and CD_3OD along with the calculated values for the minima and for the ensemble average

	A *syn*-ϕ-(+)	B *anti*-ψ	C *anti*-ϕ	D *syn*-ϕ-(−)	E non-*exo*	Ensemble average	Exp. D_2O	Exp. MeOD
H1′–HpS	2.3	1.0	3.3	1.0	11.5	2.3	1.3	1.6
H1′–HpR	11.7	10.7	3.4	9.9	3.3	10.6	9.8	8.9
H3–HpS	12.4	2.8	12.3	2.9	2.1	8.3	5.5	5.4
H3–HpR	2.5	4.2	2.1	12.3	12.3	3.9	4.1	4.8

Table 4. Relevant proton–proton distances (Å) for the population distribution ($\langle r^{-6}\rangle^{-1/6}$) and for major minima A, B and D of **1** along with the experimental values derived from NOE intensities

Proton pair	Predicted distances				Experimental
	A	B	D	Distribution	
H4–H1′	4.5	2.2	3.8	2.8	3.0
H2–H1′	3.0	2.8	4.7	3.1	3.5
H3–H1′	3.3	3.8	2.6	3.0	2.7
H2–HpR	3.8	3.3	2.4	3.1	3.0
H2–HpS	2.5	3.9	2.9	2.6	2.7
H3–HpR	2.5	2.4	3.1	2.6	Overlapping
H3–HpS	3.1	2.5	2.5	2.7	2.5
H4–HpR	2.9	3.8	2.6	2.9	2.7
H4–HpS	2.5	3.2	3.8	2.7	3.1

The first proton of the pair is the signal inverted in the 1D-NOESY experiment.

the pseudo-glycosidic are quite similar in both solvents (Table 3) suggests that only minor changes take place and that the conformational behaviour of **1** in MeOD is comparable to that in D_2O. In this regard, the NMR analysis of C-lactose revealed that the conformational behaviour of this C-analogue in DMSO-d_6 was similar to that in water, whereas some differences were detected in pyridine-d_5.[4b] The relevant inter-residue proton–proton distances in terms of the glycosidic and aglyconic angles are gathered in Table 4 for the populated conformers A, B and D, and for the distribution. It can be observed that H1′ is at a short distance from H3 in the *syn*-ψ conformers and from H4 in the *anti*-ψ conformer. Therefore, the H3/H1′ and H4/H1′ NOEs are diagnostic of the *syn*-ψ and *anti*-ψ orientations around the aglyconic bond, respectively. Both exclusive NOEs were detected in the spectra (Fig. 5), demonstrating the co-existence of both conformers in solution. Since the intensity of each NOE is sensitive to the population of the corresponding conformational family, the fact that the H3/H1′ NOE is stronger than the H4/H1′ NOE indicates, at least qualitatively, the predominance of the *syn*-ψ orientation. A more quantitative treatment was performed by comparing the distances obtained from molecular mechanics calculations with those derived from the NOE intensities using a full relaxation matrix approach.[19] It can be observed that the agreement between experimental and theoretical values is satisfactory. The major disagreements occur for H4–HpS and H2–H1′ NOEs, which are characteristic of the *syn*-$\psi(+)$ orientation, and whose intensities are weaker than those expected for the theoretical distribution. Qualitatively, this finding indicates that the population of the *syn*-$\psi(+)$ conformational family is overestimated by the calculations, as deduced also from coupling constants data. It can be estimated that a conformer distribution of ca. 40:30:30 among minima A:B:D provides the best fit to both proton–proton couplings and NOE data.

3. Conclusions

The combination of molecular mechanics and NMR studies has shown that the conformational properties of O-disaccharide **2** and its C-analogue **1** are similar

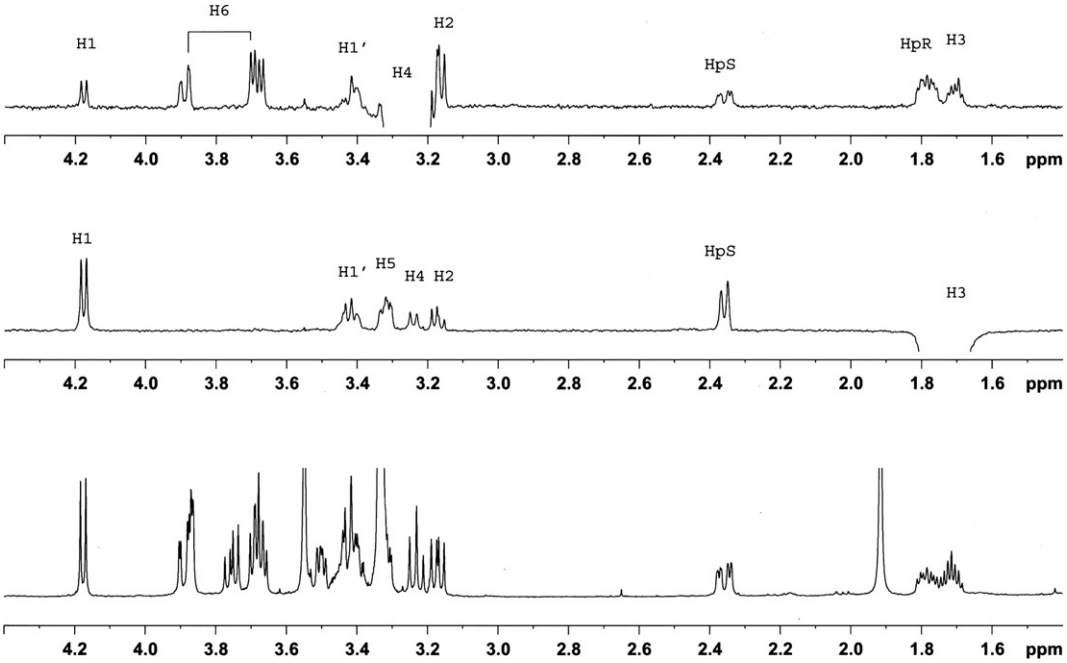

Figure 5. 1D-DPFGSE NOESY spectra of **1** (500 MHz, 298 K, CD_3OD, mixing time 500 ms) along with the ^1H spectrum. H4 and H3 resonances were inverted by using Gaussian-shaped pulses.

around the glycosidic bond, but some differences around the aglyconic bond have been found. Despite the absence of any stereo-electronic stabilization, C-disaccharide **1** adopts the *exo-syn* conformation of its parent O-glycoside. This is the same conformational preference displayed by other C-glycosides.[2,4a,b] Regarding the aglyconic bond, the *syn*-ψ conformational family is the most populated in solution. Nevertheless, the presence of the *anti*-ψ conformational family needs to be invoked to justify all the observed NOEs. The co-existence of both orientations is well predicted by the MM3* calculations. This conformational mobility around the aglyconic bond differs from that reported for the corresponding O-glycoside, in which only the *syn*-ψ conformational family was detected. The conformational differences between C- and O-glycosides described here for the β-(1→3) linkage, together with those reported for other C-/O-pairs, stress that care should be taken when using the synthetic analogues as carbohydrate models. The greater flexibility of the C-glycosides relative to O-glycosides implies a loss of entropy upon binding to a given receptor, which may be a limitation for the use of these analogues as glycosidase inhibitors. Nevertheless, these compounds are excellent probes for studying the active site of proteins.[4b]

4. Experimental

4.1. Materials

The peracetylated derivative of **1** was prepared as described.[5] This compound was treated with an excess of sodium methoxide in methanol at 25 °C for 1 h. The solution was stirred with Amberlyst, filtered and the solvent removed to afford **1**.

4.2. Molecular mechanics calculations

The relaxed (ϕ,ψ) energy maps for compounds **1** and **2** were generated by systematic rotations around the glycoside and aglyconic bond using a grid step of 18°, optimization of the geometry at every ϕ, ψ point using conjugate gradients iterations until the rms derivative was smaller than 0.05 kJ mol^{-1} Å^{-1}, and energy calculation using the MM3* force field ($\varepsilon = 80$) as integrated in MacroModel v.8.1 (Schrödinger, LLC, 2004). The *tg* and *gt* orientations of the lateral chain of the galactose moiety[20] and the *gg* and *gt* orientations of the galactose unit[21] were taken into account, because they have been shown to be much more stable than the alternative *gg* and *tg* conformers, respectively. Thus, four starting structures were considered and, in total, 1600 conformers were calculated. From these relaxed energy maps, adiabatic surfaces were built by choosing the lowest energy structure for a given ϕ, ψ point. The probability distribution was calculated for each point according to a Boltzmann function at 298 K.

4.3. *J* and NOE calculations

The vicinal coupling constants were calculated for each conformation using the Karplus–Altona equation. Ensemble average values were calculated from the distribution according to $J = \sum P_{\phi\psi} J_{i\phi\psi}$. The interproton average distances were calculated using the following expression: $\langle r^{-6} \rangle_{kl} = \sum P_{\phi\psi} r^{-6}_{kl(\phi\psi)}$. The NOE intensities were determined according to the complete relaxation matrix as described using the NOEPROM program.[22] Isotropic motion and external relaxation of 0.1 s^{-1} were assumed. A correlation time of 70 ps was used to obtain the best match between experimental and calculated NOEs for the intraresidue proton pairs H1/H3 and H1/H5.

4.4. NMR spectroscopy

NMR experiments were recorded on a Bruker Avance DRX instrument at 25 °C. A concentration of ~1 mM was used for **1**. Chemical shifts were referenced to external DSS in D_2O or to the residual signal of CD_3OD at 3.31 ppm. 1D spectra were acquired using 32 K data points, which were zero-filled to 64 K data points prior to Fourier transformation. Absolute value COSY, and phase-sensitive HSQC spectra and ROESY (mixing times of 300 and 500 ms) were acquired using standard techniques. Acquisition data matrices were defined by $2K \times 256$ points, multiplied by appropriate window functions and zero-filled to $2K \times 512$ matrices before Fourier transformation. Baseline correction was applied in both dimensions. 1D-selective NOE spectra were acquired at two different mixing times (300 and 500 ms) using the double echo sequence proposed by Shaka et al.[23] Spectra were processed using the Bruker XWINNMR program on a Silicon Graphics computer.

Acknowledgement

The CIB and ENS groups thank the PICASSO exchange programme for supporting the corresponding visits.

References

1. (a) Levy, D. E.; Tang, C. *The Chemistry of C-Glycosides*; Elsevier Science: Oxford, 1995; (b) Skrydstrup, T.; Vauzeilles, B.; Beau, J.-M. Synthesis of C-oligosaccharides. In *Carbohydrates in Chemistry and Biology*; Ernst, B., Hart, G. W., Sinay, P., Eds.; Wiley-VCH: Weinheim, 2000; Vol. 1, pp 495–530; (c) Liu, L.; McKee, M.; Postema, M. H. D. *Curr. Org. Chem.* **2001**, *5*, 1133–1167; (d) Beau, J.-M.; Vauzeilles, B.; Skrydstrup, T. C-glycosyl analogs of

oligosaccharides and glycosyl amino acids. In *Glycoscience*; Fraser-Reid, B. O., Tatsuta, K., Thiem, J., Eds.; Springer: Berlin, 2001; Vol. 3, pp 2679–2724.
2. (a) Wang, Y.; Goekjian, P. G.; Ryckman, D. M.; Miller, W. H.; Babirad, S. A.; Kishi, Y. *J. Org. Chem.* **1992**, *57*, 482–489; (b) Kishi, Y. *Pure Appl. Chem.* **1993**, *65*, 771–778; (c) Goekjian, P. G.; Wei, A.; Kishi, Y. Conformational analysis of C-glycosides and related compounds: programming conformational profiles of C- and O-glycosides. In *Carbohydrate-based Drug Discovery*; Wong, C.-H., Ed.; Wiley-VCH: Weinheim, 2003; Vol. 1, pp 305–340.
3. Jiménez-Barbero, J.; Espinosa, J. F.; Asensio, J. L.; Cañada, F. J.; Poveda, A. The conformation of C-glycosyl compounds. In *Advances in Carbohydrate Chemistry and Biochemistry*; Horton, D., Ed.; Academic Press, 2001; Vol. 56, pp 235–284.
4. (a) Espinosa, J. F.; Martín-Pastor, M.; Asensio, J. L.; Dietrich, H.; Martín-Lomas, M.; Schmidt, R. R.; Jiménez-Barbero, J. *Tetrahedron Lett.* **1995**, *36*, 6329–6332; (b) Espinosa, J. F.; Cañada, F. J.; Asensio, J.-L.; Martín-Pastor, M.; Dietrich, H.; Martín-Lomas, M.; Schmidt, R. R.; Jiménez-Barbero, J. *J. Am. Chem. Soc.* **1996**, *118*, 10862–10871; (c) Espinosa, J. F.; Bruix, M.; Jarreton, O.; Skrydstrup, T.; Beau, J.-M.; Jiménez-Barbero, J. *Chem. Eur. J.* **1999**, *5*, 442–448.
5. Vauzeilles, B.; Sinaÿ, P. *Tetrahedron Lett.* **2001**, *42*, 7269–7272.
6. Imberty, A.; Breton, C.; Oriol, R.; Mollicone, R.; Perez, S. Biosynthesis, structure and conformation of blood group carbohydrate antigens. In *Advances in Macromolecular Carbohydrate Research*; Sturgeon, R., Ed.; Elsevier, 2003; Vol. 2, pp 67–129.
7. Brown, G. D.; Gordon, S. P. P. *Immunity* **2003**, *19*, 311–315.
8. Mohamadi, F.; Richards, N. G. J.; Guida, W. C.; Liskamp, R.; Lipton, M.; Caufield, C.; Chang, G.; Hendrickson, T.; Still, W. C. *J. Comput. Chem.* **1990**, *11*, 440–467.
9. Allinger, N. L.; Rahman, M.; Lii, J. H. *J. Am. Chem. Soc.* **1990**, *112*, 8293–8307.
10. (a) Dowd, M. K.; French, A. D.; Reilly, P. J. *Carbohydr. Res.* **1992**, *233*, 15–34; (b) Imberty, A.; Mikros, E.; Koca, J.; Mollicone, R.; Oriol, R.; Perez, S. *Glycoconjugate J.* **1995**, *12*, 331–349.
11. Kony, D.; Damm, W.; Stoll, S.; Hunenberger, P. H. *J. Phys. Chem. B* **2004**, *108*, 5815–5826.
12. French, A. D.; Kelterer, A.-M.; Johnson, G. P.; Dowd, M. K.; Cramer, C. J. *J. Mol. Graphics Modell.* **2000**, *18*, 95–107.
13. Sagas, P.; Bush, C. A. *Biopolymers* **1990**, *30*, 1123–1138.
14. Tvaroska, I.; Hricovini, M.; Petrakova, E. *Carbohydr. Res.* **1989**, *189*, 359–362.
15. Cheetham, N. W. H.; Dasgupta, P.; Ball, G. E. *Carbohydr. Res.* **2003**, *338*, 955–962.
16. Dabrowski, J.; Kozar, T.; Grosskurth, H.; Nifant'ev, N. E. *J. Am. Chem. Soc.* **1995**, *117*, 5534–5539.
17. Mikros, E.; Labrinidis, G.; Pérez, S. *J. Carbohydr. Chem.* **2000**, *19*, 1319–1349.
18. Haasnoot, C. A. G.; de Leeuw, F. A. A. M.; Altona, C. *Tetrahedron* **1980**, *36*, 2783–2792.
19. Neuhaus, D.; Williamson, M. P. *The Nuclear Overhauser Effect in Structural and Conformational Analysis*; VCH: New York, 1989.
20. Kroon-Batenburg, L. M. J.; Kroon, J. *Biopolymers* **1990**, *29*, 1243–1248.
21. Mackie, D. M.; Maradufu, A.; Perlin, A. S. *Carbohydr. Res.* **1986**, *150*, 23–33.
22. Martín-Pastor, M. Ph.D. Thesis, Universidad Autonoma, Madrid, 1997.
23. Stott, K.; Stonehouse, J.; Keeler, J.; Hwang, T.-L.; Shaka, A. J. *J. Am. Chem. Soc.* **1995**, *117*, 4199–4200.